OPEN ACCESS

chromatography

Review

Post-Polymerization Modifications of Polymeric Monolithic Columns: A Review

Sinéad Currivan and Pavel Jandera *

Department of Analytical Chemistry, Faculty of Chemical Technology, University of Pardubice, Studentská 573, Pardubice 532 10, Czech Republic; E-Mail: sineadann.currivan@upce.cz

* Author to whom correspondence should be addressed; E-Mail: pavel.jandera@upce.cz;
Tel.: +420-460-037-023.

Abstract: The vast cache of methods used in polymeric monolithic column modification is presented herein, with specific attention to post-polymerization modification reactions. The modification of polymeric monolithic columns is defined and can include the modification of pre-existing surface groups, the addition of polymeric chains or indeed the addition of structures such as nano-particles and nano-structures. The use of these modifications can result in the specific patterning of monoliths, useful in microfluidic device design or in the investigation of modification optimization.

Keywords: polymer monoliths; modifications; HPLC; CEC; grafting; click chemistry; hypercross-linking; nano-particles

List of Abbreviations: 2-acrylamido-2-methyl-1-propanesulphonic acid AMPS, α, α'-azoisobutyronitrile AIBN, adenosine triphosphate ATP, atom transfer radical polymerization ATRP, benzoyl peroxide BPO, bovine serum albumin BSA, butyl methacrylate BuMA, capillary electrochromatography CEC, capillary electrophoresis CE, cyclic olefin copolymer COC, 2,2-dimethoxy-2-phenylacetophenone DAP, dichlorethane DCE, dimethyl formamide DMF, divinyl benzene DVB, ethyleneglycol dimethacrylate EDMA, electroosmostic flow EOF, green fluorescent protein GFP, glycidyl methacrylate GMA, gold nano-particle(s) AuNP(s), hydroxyethyl methacrylate HEMA, hydrophilic interaction liquid chromatography HILIC, iminodiacetic acid IDA, isocyanoethyl methacrylate IEM, iron oxide nano-particle(s) IONP(s), lauryl methacrylate LMA, N,N-dimethyl-N-methacryloxyethyl-N-(3-sulfopropyl) ammonium betaine MEDSA, methacryloyloxyethyl trimethylammonium chloride

META, methyl methacrylate MMA, 4-methyl styrene MST, multi-walled carbon nano-tube(s) MWCNT(s), N-acryloxysuccinimide NAS, nano-flower(s) NF(s), oligoethylene glycol OEG, polyethyleneglycol methacrylate PEGMA, polyethylimine PEI, polymer monolith micro-extraction PMME, Teflon PTFE, reversible addition-fragmentation chain transfer RAFT, reversed-phase RP, ring opening metathesis polymerization ROMP, scanning capacitively coupled contactless conductivity detection sC^{4}D, scanning electron microscope SEM, silver nano-particle(s) SNP(s), solid phase extraction SPE, sulphopropyl methacrylate SPM, styrene STY, 2,2,6,6-tetramethylpiperidyl-1-oxy TEMPO, trimethylolpropane trimethacrylate TRIM, vinyl azlactone VAL, vinylbenzyl chloride VBC.

1. Introduction

Organic polymer monolithic columns were first devised by Hjertén in the late 1980s [1] and further developed throughout the early 1990s [2–5]. Porous polymer rods have come to include sophisticated column designs for columns and microfluidic devices, which contain not only multifunctional surface chemistries [6–9], but also differing concentrations of surface functionality [10–13], separate to the column morphology. Many reviews regarding monolith fabrication have been written since the inception of polymeric monoliths, with focused reviews on preparation [14–18], modification [19–22], and with special consideration of particular applications such as ion exchange [19,20], solid phase extraction [22,23], biomolecule immobilization [22,24–26], and the role of nano-particles in biomolecule immobilization [27]. This review is aimed at highlighting categories of post-polymerization modifications available for polymeric monolithic columns, prepared by free radical polymerization via thermal or UV initiated methods.

In recent years, the use of post-polymerization modification has become a commonplace technique in the preparation of monolithic separation media. The goal of post-polymerization modifications is to separate the control of morphology from the selectivity, modification, and tailoring of the surface chemistry [28]. This type of modification can result in the use of monoliths with readily optimized morphologies, as well as increased surface density of desired functional groups leading to increased efficiency [7,28]. The most technically straightforward method to incorporate the desired surface functionality is to co-polymerize a desired monomer with a cross-linker, and/or a second functional monomer [4,5,11,28,29]. Monolithic columns prepared directly from a monomer of desired functionality and a cross-linker also have been reported [30–35]. Co-polymerization is a well-established method for the preparation of monolithic columns expressing the desired chemistry [28], however, as polymeric monoliths express a high population of large through-pores, they have limited surface areas, and as such can express a low surface availability of functional groups [2]. The available surface functionality can be limited, as monomers with specific functionality may not always be commercially available, and synthesis may not be a viable option [15]. To generate these specific surface chemistries, columns have been subsequently modified following preparation of a "generic" base monolith [36–38]. Using a number of techniques, such as reactions with pendant surface groups, grafted chain growth, hypercross-linking, or indeed with the introduction of nano-structures to the formed monolith, the desired surface functionality can be tailored. Post-polymerization modification can be defined as those reactions limited to the surface of the monolithic column, using (a) reaction chemistry (e.g., glycidyl methacrylate (GMA), N-acryloxysuccinimide (NAS), vinyl azlactone (VAL))

from a functional group incorporated into the monolith structure; (b) grafting of additional polymer layers by means of thermal or photo-initiated polymerizations; or (c) the addition of nano-architectures to aid in selectivity or to enhance surface area.

A reactive monomer such as GMA [2,3], VAL [5,6,11,39], or NAS [40–43], can be incorporated into the monolithic matrix, which can be further modified to express a preferred surface chemistry. Since the introduction of rigid monolithic columns [2], GMA has been used as a co-monomer in monolithic column preparations with varying modification reactions performed *in situ*. The reactive GMA group is generally used to convert monolithic columns to ion exchange selectivity [2,28,44–51], affinity selectivity [52–56] or, for the immobilization of zwitterionic molecules, for other protein separations [57–59]. Such columns can find applications in microLC, capillary electrophoresis (CE), or capillary electrochromatography (CEC). This method of modification is known for its relative ease in preparation, however, Svec reports that it generally yields a low surface coverage, as the reliant chemical group (e.g., oxirane) is not only expressed sporadically on the globular surface of the monolith, but is also inaccessible within the bulk of the globule [15]. Compared to a secondary polymerization approach, e.g., grafting, wherein a network of new functional groups can be generated, this reaction chemistry results in the conversion of only the available reactive sites, generated by the initial polymerization procedure. This was further emphasized by Rohr *et al.* who noted that the use of potential reactive sites on the surface of the monolith for further modification was first dependent on the primary coverage of such sites [37]. To increase the surface density, using this co-polymerization method, the alteration of the monolith components (such as monomer concentration and porogen ratios) would be required, which, thus, results in significant changes in the monolith morphology [37]. A number of excellent recent reviews on the merits of co-polymerized stationary phases have been published [16–21,23], and the reader may be directed there for further detail.

2. Photo-Grafting Reactions

Using reactive sites latent in the monolith structure, such as those described above, does not afford a precise control over functionalization, where precise spatial control is required (e.g., in the preparation of monolithic media microfluidic devices [7]). As useful as co-polymerization may be, the availability of surface groups still remains problematic [15,37]. Graft polymerization involves the growth of polymer chains from the surface of a solid support, such as a polymeric monolithic column [7,37]. Photo-initiated grafting procedures were investigated, stemming from the seminal work of Rånby *et al.* [60–65], following the innovation of photo-initiated polymerizations in 1997 [66]. Photo-initiated polymerizations and grafting offer enhanced flexibility relative to co-polymerization of monomers for dedicated chemistries. The available grafting procedures are overviewed in tables in the maintext. Photo-grafting has many uses, including the implementation of a number of different functionalities on the surface of a monolith substrate, as demonstrated in Figure 1. Using photo-grafting, a dense polymeric network can be formed upon a substrate, thus shielding the underlying functionality of the substrate, and resulting in a separate functionality at the surface [29,36,67,68].

Figure 1. Schematic of single step photo-grafting of a grafted zone upon a preformed monolithic column.
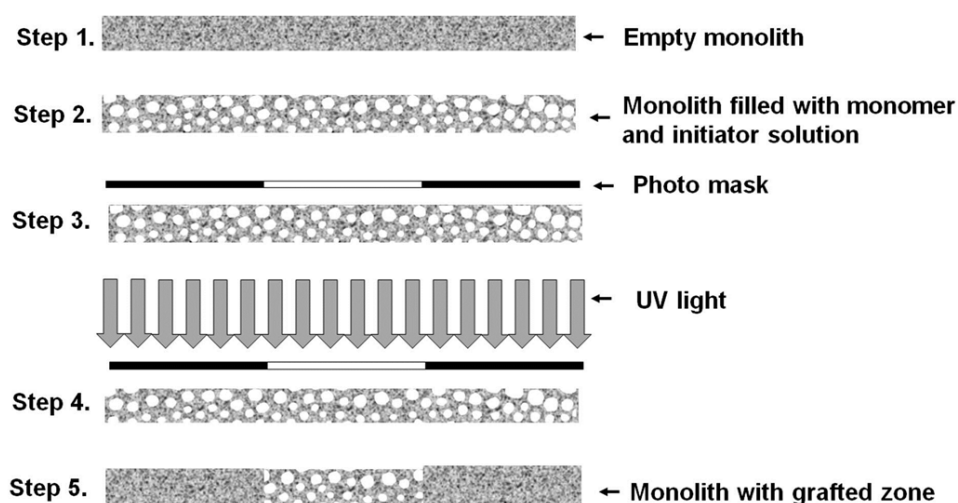
Some photo-grafting techniques specifically used a single step in grafting procedures, *i.e.*, initiator and monomer present simultaneously within the column. When a single grafting step is used, polymerization occurs not only from the monolith's surface as desired, but also in solution within the pores of the monolith [7]. As a result, solution localized polymerizations form a viscous gel, which may be difficult to remove. The method of photo-grafting was improved upon by Stachowiak *et al.*, wherein a multi-step grafting procedure using benzophenone was developed [7], as shown in Figure 2. The new protocol involved the immobilization of the initiator to the monolith's inner surface, by using photo-induced lysis, leaving a surface bound free radical. The UV irradiation procedure causes excitation of the electrons within the polymer, with consequential hydrogen abstraction from the polymer surface. In the absence of monomers, the surface bound radical binds to the semi-pinacol radical formed by the absorption of UV energy by benzophenone. In the presence of monomers and a secondary exposure to UV energy, the initiator is liberated from the surface, dimerizing in solution, exposing the surface bound free radical for graft chain growth. In using this method, the efficiency of grafting can be enhanced, as fewer monomer molecules are "lost" to solution located chain growth. This technique also reduces the viscosity of free/unreacted materials subsequently removed from the column.

Figure 2. Two step sequential grafting, upon a preformed monolithic column, using benzophenone as the photo-initiator. Reprinted with permission from [7]. Copyright 2006 American Chemical Society.
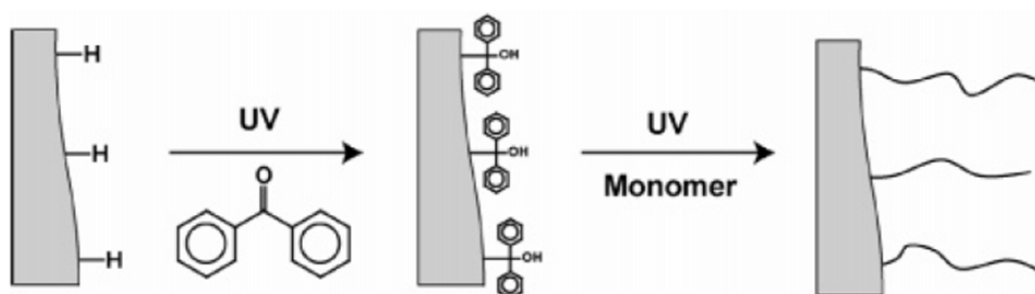
2.1. Monolithic Columns Grafted with Ionizable Exchange Groups

Photo-grafting for uses in HPLC and CEC was developed by Rohr *et al.* in 2003 [36,37]. Firstly, a charged monomer 2-acrylamido-2-methyl-1-propanesulphonic acid (AMPS) was grafted to the surface of a "generic" poly(butyl methacrylate-*co*-ethyleneglycol dimethacrylate) (poly(BuMA-*co*-EDMA)) monolithic column [37]. The effect of grafting time was investigated, with an increased pressure drop on the monolithic column, resulting from an increase in graft time. This was indicative of the growing dense network of polymer chains, with increasing irradiation time. The electroosmostic flow (EOF) was generated by the charged AMPS graft. In CEC, the EOF was found to plateau once a certain density of grafts was achieved, as only those sites at or near to the surface contribute to EOF. Photo-patterning (the photo-grafting of selective groups in defined areas) was also investigated, where reactive VAL groups were grafted to a "generic" monolith. Fluorescent rhodamine 6G was covalently attached to the VAL sites, enabling a visual cross-validation of "patterned" sites. Using a fluorescence-based assay, an increased fluorescent intensity was observed for a column grafted with the same irradiation intensity for a longer period of time.

Connolly *et al.* grafted methacryloyloxyethyl trimethylammonium chloride (META) to a poly(GMA-*co*-EDMA) monolithic column to prepare a grafted anion exchange selectivity [69], using a single step graft polymerization with benzophenone as the initiator. The column was capable of delivering efficiencies of up to 29,500 N/m (for inorganic anions) at a reduced flow rate of 100 nL/min, higher than the latex agglomerated (quaternary ammonium-functionalized) monolithic columns described by Hilder *et al.* (26,000 N/m), which were prepared via co-polymerization with nano-particle modification [46].

Improved photo-grafting was accomplished using multi-step initiator immobilization with subsequent grafting by Stachowiak *et al.* [7]. Eeltink *et al.* used a single step in the surface modification of neutral monolithic columns (poly(BuMA-*co*-EDMA)) with ionized functional monomer, either AMPS or META [67]. Measurements on pre- and post-modified monoliths have shown that the grafting procedure supported the generation of EOF. Increasing the amount of grafting functional monomer in solution (META) from 0.5% to 15% resulted in a ten-fold increase in electro-osmotic mobility. In addition, the group investigated the increased retention of hydrophobic analytes in reversed-phase (RP) CEC. An ionizable layer (META) was grafted to the monolith, followed by 10 min of grafting of a hydrophobic monomer lauryl methacrylate (LMA), leading to a 53% increase of the retention factor in reversed-phase CEC, in agreement with the findings by Rohr *et al.* [37], and Hilder *et al.* [36].

Changes to surface chemistry following grafting procedures were investigated by Connolly *et al.* [70], where they grafted discrete zones of ionized AMPS to a neutral poly(BuMA-*co*-EDMA) monolithic column. Using a contactless conductivity detector (scanning C^{4}D, sC^{4}D), the relative density of the grafted zones could be mapped, providing a cross-validation of the grafting procedure. Grafted zones of VAL were also produced to immobilize histidine-tagged green fluorescent protein (GFP). Similarly, Gillespie *et al.* studied the fundamentals in photo-grafting behavior, using poly(AMPS) grafts on poly(BuMA-*co*-EDMA) monolithic columns, whilst using sC^{4}D as a characterization technique [29]. The zones of grafted charged monomer were subjected to varying doses of UV energy, and thus density of grafted chains. The detector's response was proportional to the amount of charged monomer grafted in the column, however, it was noted that a plateau in detector response occurred with

increased UV doses. This is supported by the observations made by Hilder *et al.* [36,67], wherein the uppermost layer is attributed to the resulting charge density. In addition, the group also demonstrated that a minimum UV dose was required to initiate the photo-grafting step, as doses below 1 J/cm^2 UV energy (in this case) resulted in no change of detector response across that zone relative to the baseline monolith.

2.2. Grafted Monolithic Columns for Biomolecule Immobilization

The immobilization of a biomolecule to the polymeric monolithic surface may firstly require the hydrophilization of the monolith's surface [8,13,71–73] by grafting a neutral hydrophilic monomer [7]. Peterson *et al.* prepared a dual function monolith incorporating a μ-solid phase extraction (SPE) section, followed by an enzymatic reactor [68]. A generic hydrophobic monolith was prepared (poly(BuMA-*co*-EDMA)), to which a 20 mm section of monolith was grafted with VAL for further reaction with trypsin, thus creating the enzymatic reactor segment of the monolith. The remaining length of the hydrophobic monolith was dedicated to μSPE. In addition, a co-polymerized monolith incorporating VAL was also prepared (poly(EDMA-*co*-2-hydroxyethyl methacrylate-*co*-VAL)). The photo-grafted and co-polymerized columns exhibited similar porosity, and so were compared directly. The photo-grafted column demonstrated a higher enzymatic activity compared to the co-polymerized monoliths. The effect of time upon the graft density was investigated and measured by enzymatic activity. Increasing graft time showed a proportional increase in graft density and a pressure drop across the column within the limits of the experiment, *i.e.*, between 1 and 3 min of grafting. The column was used successfully in the digestion of a peptide consisting of fluorescent fragments, facilitating the visualization of the SPE zone. Logan *et al.* produced a column expressing three segments of differing enzymatic systems, each specifically placed using photo-grafting of the reactive monomer, VAL [8]. The monolith (poly(BuMA-*co*-EDMA)) was grafted first with polyethyleneglycol methacrylate (PEGMA) along the column, producing a hydrophilized surface. Sequential grafting of three discreet zones of VAL was used to immobilize each of the enzymes (glucose oxidase, horseradish peroxidise, and invertase). Using VAL grafts and green fluorescent protein (GFP), the group determined that the use of sequential grafting had little or no effect on the activity of the initially immobilized GFP, and thus immobilized enzymes. This demonstrates the versatility of the photo-masking technique to graft monolithic columns within a single column housing, with a variety of different functionalities via subsequent steps.

Monomers such as acrylamide, vinyl pyrrolidinone, 2-hydroxyethyl methacrylate (HEMA), and polyethyleneglycol methacrylate (PEGMA) were grafted upon poly(BuMA-*co*-EDMA) monoliths in an effort to study their resistance to protein adsorption [7]. Fluorescent bovine serum albumin (BSA) and GFP were flushed across the test columns, where zones of hydrophilic monomer were grafted, resulting in a fluorescent pattern across the column. On the non-grafted sections of the monolith, the protein probes were adsorbed, and the grafted monomers showed reduced fluorescence intensity (HEMA and PEGMA only). The fluorescence assay provided a qualitative validation of the grafted groups, both in location and ability to resist protein adsorption. The cross-validation of grafted moieties was also probed by Connolly *et al.* [70], wherein poly(VAL) grafts were generated on the surface of poly(BuMA-*co*-EDMA) monolithic columns. The grafts facilitated the immobilization of

GFP for fluorescent visualization and also bovine serum albumin. The spatial location of these groups was visualized non-destructively using the fluorescence of immobilized GFP and sC⁴D profiling. Using the sC⁴D technology, the zones of grafted moieties were easily confirmed and visualized.

Křenková *et al.* used photo-grafting to introduce hydrophilic surface chemistry to an otherwise hydrophobic monolithic column [71], similar to the work by Stachowiak *et al.* [7], and Logan *et al.* [8]. In the report, poly(PEGMA) chains were grafted to poly(GMA-*co*-EDMA) monolithic columns to reduce the adsorption of hydrophobic proteins to the surface. In a secondary grafting step, VAL was grafted to facilitate the immobilization of trypsin and endoproteinase LysC for enzymatic digestion. The first grafting step of poly(PEGMA) to poly(GMA-*co*-EDMA) monoliths required the hydrolysis of the epoxide rings prior to the immobilization of benzophenone. Using a fluorescence assay, the non-specific adsorption of BSA was visualized before and after grafting. The grafting of poly(PEGMA) resulted in a significant decrease in fluorescence intensity. The enzymatic reactor columns (both trypsin and endoproteinase LysC) were used in the successful digestion of a number of proteins with mass spectra obtained for the digested peptide fragments. Similarly, hydrophilization was repeated for this group [72], for the immobilization of PNGase F, in the analysis of glycoproteins, wherein a multi-step grafting procedure was used. A secondary column was used for the subsequent separation of the peptide fragments.

2.3. Monolithic Columns with Bonded Ligands

Boronate affinity phases are used to selectively extract molecules with 1,2- and 1,3-*cis*-vicinal diols, which are common to most carbohydrates [73]. Potter *et al.* used two approaches in the preparation of boronic acid columns and compared both co-polymerization of GMA and photo-grafting of poly(GMA) grafts to a monolith surface [73]. The boronate affinity columns demonstrated the retention of ribonucleosides, with an increased affinity in the photo-grafted column. This was due to an increase in the surface density of grafted polymer chains [29] relative to the sporadic nature of co-polymerized co-monomer [28].

Gillespie *et al.* prepared generic poly(BuMA-*co*-EDMA) monolithic columns, to which zones of *m*-aminophenyl boronic acid were immobilized in two spatially discrete areas via poly(VAL) grafts [74]. The column was also subjected to the grafting of PEGMA in order to reduce non-specific binding [7] prior to VAL grafting and attachment of the boronate ligand. Using sC⁴D techniques, a study was performed into the pK_a of immobilized boronate ligand following its immobilization using a range of pH buffers. Later, the group performed another investigation of pK_a of aminocarboxylates following immobilization on grafted VAL sites [75]. The pK_a of the immobilized acids were shifted from those reported in the literature for bulk solutions. This work demonstrates that photo-grafting can be exploited for the investigation of the fundamental properties of immobilized functional groups.

The use of UV initiating techniques is limited by the composition of monolithic column housing materials. For *in situ* polymerizations, fused silica capillaries coated in Teflon (PTFE) are generally used for UV-initiated procedures, but diameters greater than 250 μm are not widely available. Polyimide coated capillaries are widely available and cheaper than their PTFE counterparts. Walsh *et al.* used light at a wavelength of 470 nm to initiate the polymerization of poly(styrene-*co*-divinyl benzene) (poly(STY-*co*-DVB)) monolithic columns within PTFE coated capillaries [76]. Later, an in-house

prepared spiropyran monomer was grafted to the surface of poly(BuMA-*co*-EDMA) monolithic columns in polyimide coated capillaries using light initiation at 660 nm [77] (see Table 1).

Table 1. Reactions used in the production of photo-grafted stationary phases.

| Monolith	Reaction	Graft energy	Time	Reference
Poly(BuMA-co-EDMA)	Single and sequential two step grafting of monomers.	500 W	60 * min	[7]
Poly(BuMA-co-EDMA)	Sequential grafting of PEGMA and VAL.	500 W	60 * min	[8]
Poly(BuMA-co-EDMA)	Single step grafting of gradients of AMPS.	500 W	1 to 10 min	[10]
Poly(BuMA-co-EDMA)	Single step grafting of gradients of AMPS.	3 J/cm^2	N/A	[11]
Poly(BuMA-co-EDMA)	Sequential grafting of PEGMA, VAL, and SPM.	1 J/cm^2 each step	N/A	[13]
Poly(BuMA-co-EDMA)	Single step grafting of AMPS.	0.25 to 7 J/cm^2	N/A	[29]
Poly(BuMA-co-EDMA)	Single step grafting of AMPS and butyl acrylate.	500 W	0.5 to 1.5 min	[36]
Poly(BuMA-co-EDMA)	Single step grafting of AMPS and VAL.	500 W	30 min	[37]
Poly(BuMA-co-EDMA)	Single step grafting of META and butyl acrylate.	1.4 mW/cm^2	3 min	[67]
Poly(BuMA-co-EDMA)	Single step grafting of VAL for dual function monolith.	15 mW/cm^2	3 min	[68]
Poly(GMA-co-EDMA)	Single step grafting of META.	0.25 J/cm^2	N/A	[69]
Poly(BuMA-co-EDMA)	Single step grafting of AMPS and VAL.	N/A	60, 30 min respectively	[70]
Poly(GMA-co-EDMA)	Sequential grafting of PEGMA and VAL.	12 mW/cm^2	4 * 1 to 6 min (VAL)	[71]
Poly(BuMA-co-EDMA) and Poly(GMA-co-EDMA)	Sequential grafting of PEGMA and VAL.	N/A	4 *, 2 min	[72]
Poly(BuMA-co-EDMA)	Sequential grafting of PEGMA and VAL.	3 * J/cm^2	N/A	[74]
Poly(BuMA-co-EDMA)	Single step grafting of VAL.	3 J/cm^2	N/A	[75]
Poly(BuMA-co-EDMA)	Single step grafting of spiropyran monomer using VIS LED at 660 nm.	0.5 cd	2 min	[77]
Poly(LMA-co-EDMA)	Multi step grafting of VAL.	1 * J/cm^2	N/A	[78]
Poly(LMA-co-EDMA)	Multi step grafting of GMA.	1 * J/cm^2	N/A	[79]

* Each step *i.e.*, initiator immobilization and subsequent grafting reaction.

The use of chelate immobilized monolithic columns has so far been restricted to the ring opening reactions of GMA in GMA supported monoliths, but few rely on surface grafting [13,52,75]. Moyna *et al*. prepared poly(LMA-*co*-EDMA) monolithic columns with subsequent poly(VAL) grafts [78]. Chelating ligands, such as iminodiacetic acid (IDA) and acetyl-iminodiacetic acid, were immobilized via the poly(VAL) grafted chains. The resulting columns demonstrated efficiencies lower than 5,000 N/m, however, enhanced selectivity was evident. In a second report [79], Moyna *et al*. grafted poly(LMA-*co*-EDMA) monolithic columns with the epoxide containing a GMA monomer, which was subsequently used for IDA immobilization. The column was used in the separation of transition metals in seawater samples, however, the efficiency although improved from poly(VAL) grafts [79], was still relatively low, at 5,070 N/m.

2.4. Monolithic Columns Grafted with Heterogeneous Grafting Energies

In UV initiated grafting, the density of the graft can be altered using UV energy, time of irradiation, and concentration of the monomer/initiator. As first described by Rohr *et al*. [37], the use of filters could produce a grafted gradient of functional monomer, where the grafting efficiency increases with increasing light exposure for grafting [37,80]. In order to create a grafted gradient of functionality upon a homogeneous monolith, Pucci *et al*. prepared poly(BuMA-*co*-EDMA) monolithic columns, which were later modified with AMPS using a number of different methods [10]. Three methods of grafting were investigated using single step modification. The successful method included a polymer film to reduce the intensity of the UV source, whilst a moving shutter changed the temporal exposure of the column. By reducing the intensity of light, a longer irradiation time could be used, resulting in a lower chance of experimental error and increased reproducibility. From the three columns prepared, the greatest column efficiency was achieved with 85,900 N/m in the CEC separation of salicylic acid and acetyl salicylic acid. A comparison of the gradient columns is shown in Figure 3.

Figure 3. (**a**) Chromatograms generated on an isotropic column, (**b**) a gradient prepared using a moving shutter, and (**c**) a gradient produced using a neutral density filter. Analytes ASA = acetylsalicylic acid, SA = salicylic acid. Mobile phase 80:20 ACN:10 mM phosphate buffer pH 2.5. Separation voltage = 25 kV, electrokinetic injection at 5 kV for 5 s. UV detection at a wavelength of 200 nm.
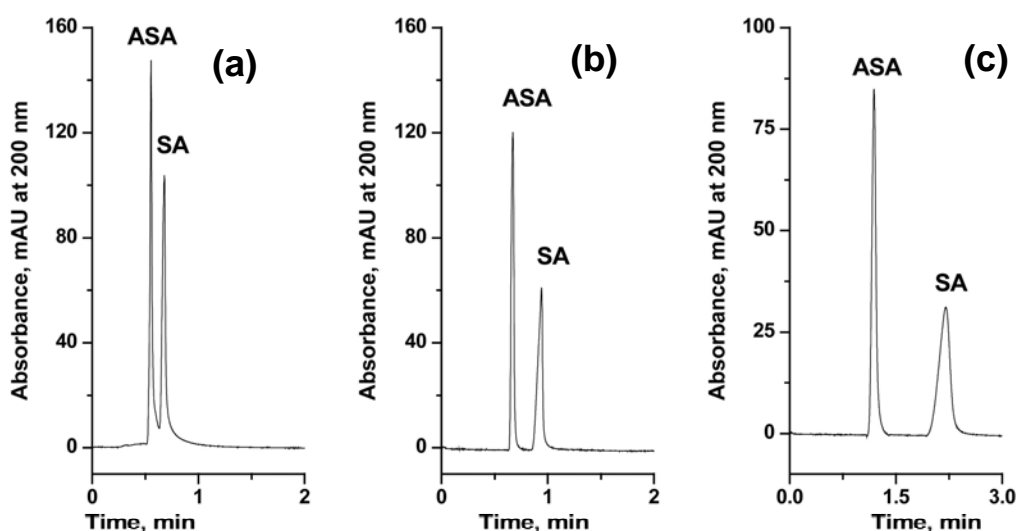
Similar to the work performed by Pucci *et al*. [10], Currivan *et al*. prepared gradients of grafted functionality of AMPS upon a poly(BuMA-*co*-EDMA) monolithic column, using a commercially available neutral density gradient filter [11]. The distribution of the gradient was also characterized using sC^{4}D profiling, which provided qualification of the gradient indirectly. However, the attenuation of the filter was too great due to an excessive absorbance. Currivan *et al*. later produced a grafted stationary phase gradient, which was fabricated using commercially available cyclic olefin copolymer (COC) films [13].

The gradient of functionality was prepared upon otherwise neutral poly(LMA-*co*-EDMA) monoliths, some of which had been subjected to hydrophilization with PEGMA grafting. The ease in

tailoring the material to the absorbance range made it an attractive method for UV light attenuation. The columns were modified using poly(VAL) for IDA immobilization, and poly(SPM) grafted chains. The strong cation exchange column was used in the separation of lysozyme and transferrin, with a decrease in peak width of 26%, demonstrating a peak focusing ability of this technology. The presence of the gradient was verified using sC^{4}D profiling.

3. "Click" Chemistry

An emerging technique for *in situ* post-polymerization modification of monolithic columns has been developed by a technique used originally in organic synthesis [81]. The technique has been used on silica and hybrid silica-polymeric monolithic columns [81–86], however, this is beyond the scope of the current review. Click reactions include alkyne-azide, thiol-ene, and thiol-yne reactions [81] and may be conducted using elevated temperatures or at ambient room temperature. Click modification reactions occur in the presence of water and oxygen, unlike many polymer graft reactions, wherein molecular oxygen must be removed prior to polymerization [81]. For reactions occurring at room temperature, a metal catalyst is used. Some reactions are completed in the presence of an initiator such as AIBN or 2,2-dimethoxy-2-phenylacetophenone (DAP). In these techniques, a surface thiol is required. Preparation methods can be seen in Table 2.

Table 2. Reactions used in "click" chemistry immobilization strategies.

| Monolith	Reaction	λ (nm)	Temperature (C°)	Time	Reference
Poly(NAS-*co*-EDMA)	Propargylamine modification to produce surface alkyne. Click grafting of 1-adamantanethiol using UV irradiation at 313 nm, using darocure as initiator.	313	N/A	30, 60, 120, and 180 min	[43]
Poly(GMA-*co*-EDMA), Poly(GMA-*co*-MMA-*co*-EDMA), Poly(GMA-*co*-HEMA-*co*-EDMA)	Surface sulfhydryl groups clicked with (S)-N-(4-allyloxy-3,5-dichlorobenzoyl)-2-amino-3,3-dimethylbutanephosphonic acid in the presence of AIBN initiator.	N/A	60	24 h	[50]
Poly(GMA-*co*-EDMA)	Surface thiol groups clicked with O-9-tert-butylcarbamoylquinine in the presence of AIBN.	N/A	60	24 h	[87]
Poly(IEM-*co*-MMA-*co*-EGDMA)	Monoliths modified with 1-octanol, 1-decanol, 1-dodecanol, 1-octadecanol, n-decylamine and 1-decanethiol.	N/A	60	N/A	[88]
Poly(GMA-*co*-EDMA)	Monolith thiolated with cysteamine, with cleavage of the disulphide thus exposing thiols. MEDSA or LMA clicked using either heat or UV initiation.	360	80	N/A	[89]
Poly(NAS-*co*-EDMA)	Allylamine modified monolith surface reacted with 1-octadecanethiol in the presence of AIBN and UV initiation.	365	N/A	4 h	[90]

Table 2. *Cont*.

Monolith	Reaction	λ (nm)	Temperature (C°)	Time	Reference
Poly(propargyl methacrylate-*co*-EDMA)	Click addition of 1-azidooctane and 1-azidooctadecane using a Cu(I) catalyst.	N/A	30	120 h	[91]
Poly(GMA-*co*-EDMA) and poly(VBC-*co*-DVB)	Azide modified surfaces clicked with 1-decyne using a Cu(I) catalyst.	N/A	30 to 60	48 h	[92]
Poly(3-(Trimethoxysilyl)propyl acrylate-*co*-propargylacrylate-*co*-AMPS-*co*-TRIM-*co*-PETRA)	Active surface modified with cinnamidyl azide or 6-azido-6-deoxy-beta-cyclodextrin.	N/A	84	16 h	[93]

3.1. Thiol-Ene Click Reactions in Monolithic Column Functionalization

Preinerstorfer *et al*. prepared poly(GMA-*co*-EDMA) monolithic columns for chiral selector modification (see Figure 4) [87]. The column was successfully used in the separation of *N*-3,5-dinitrobenzoyl-leucine enantiomers, however, relatively low efficiencies were obtained (figures not published) and attributed to the inherent macro-porosity of the monolithic porous structure. Later, the monoliths were used for thiol functionalization [50]. The available content of epoxide groups was only 10%, due to the incorporation of the large majority of epoxides within the monolith structure, as reported by Sýkora *et al*. [44]. The column was employed for the separation of enantiomers of mefloquine tert-butylcarbamate, with the highest efficiency obtained for an eluent containing 20% methanol (MeOH) (>47,000 N/m).

Figure 4. Schematic of a thiol-ene click reaction, with radical (AIBN) addition of O-9-tert-butylcarbamoylquinine to the available surface bound thiol groups. Reprinted from [87]. Copyright (2004), with permission from Elsevier.
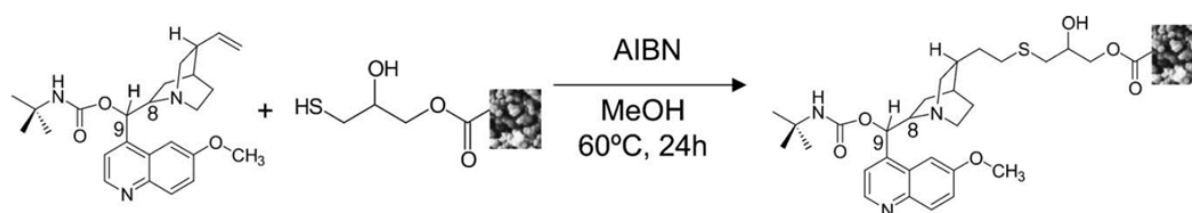
Lv *et al.* produced poly(isocyanoethyl methacrylate-*co*-methyl methacrylate-*co*-EDMA) monoliths (poly(IEM-*co*-MMA-*co*-EDMA)) to facilitate modification using hydroxyl, amine, or thiol functionalities [88]. The longer the alkyl chain length of the respective modifier, the lower was the ligand density. Later, using poly(GMA-*co*-EDMA) monoliths, thiol-ene reactions were performed in both UV and thermal initiated addition reactions. A reversed-phase column (LMA) and a hydrophilic interaction liquid chromatography (HILIC) column (N,N-dimethyl-N-metacryloxyethyl-N-(3-sulfopropyl) ammonium betaine, MEDSA) were produced upon thiolated columns [89]. The UV initiation method outperformed the thermal initiation with a ten-fold increase in plate count for uracil (3,000 N/m to 30,000 N/m, respectively), and a lower pressure drop across the column. A zwitterionic column was prepared using a betaine type methacrylate providing an efficiency of 19,000 N/m for guanosine in the

separation of nucleotides, which was greater than the column prepared by direct co-polymerization of MEDSA and EDMA [30].

Tijunelyte *et al.* [90] prepared a poly(NAS-*co*-EDMA) monolithic column, modified with allylamine, after which thiolated oligoethylene glycol (OEG) was grafted to the column via surface alkene groups, *i.e.*, thiol-ene clicking. A yield of 50% was achieved due to the large size of OEG units. The column was used in the separation of DMF, acrylamide, and toluene and showed dual retention mechanisms dependent on the percentage of organic modifier in the mobile phase, typical of HILIC columns. Additionally, a reversed-phase (RP) column was prepared using the thiol-ene click pathway, resulting in a C_{18} bonded stationary phase.

3.2. Thiol-Yne Click Reactions in Monolithic Column Functionalization

Dao *et al.* used UV initiation at 313 nm to click adamantanethiol to the surface of propargylamine modified poly(NAS-*co*-EDMA) monoliths [43]. A solution of 0.5 *M* 1-adamantanethiol (in MeOH) and the initiator darocure (10% w.r.t. adamantanethiol concentration) were pumped across the column. Sun *et al.* produced a monolithic column with direct co-polymerization of the alkyne monomer propargyl methacrylate and EDMA [91]. The pendent alkyne functionalities were further reacted with in-house synthesized azides (1-azidooctane, 1-azidooctadecane). A number of proteins were separated using the two modified columns, with flow rate experiments also conducted on the C_{18} column. In a later report, Sun *et al.* used poly(GMA-*co*-DVB) and poly(vinylbenzyl chloride-*co*-DVB) monoliths for alkyne cyclo-addition [92]. Increasing the reaction temperature resulted in an increase in yield from ~30% to 100%.

Salwinski *et al.* produced poly(propargyl acrylate-*co*-pentaerythritole triacrylate-*co*-AMPS-*co*-trimethylolpropane trimethacrylate) monolithic columns for applications in CEC [93]. The columns were modified via pendent alkyne functionalities on the monolith inner surface. Using 6-azido-6-deoxy-β-cyclodextrin and cinnamyl azide, the columns were modified, after which the EOF decreased due to the formation of additional layers on the monolith's inner surface, resulting in a shielding effect for AMPS, which is the source of EOF, which is also noted in graft polymerization reactions [29,36].

4. Thermally Initiated Graft Chain Growth

The use of thermally initiated graft polymerization was first reported for monolithic columns in 1997. Peters *et al.* produced a monolithic column with thermally grafted polymer chains, which exhibited thermal responsive behavior [38]. Two types of thermal responsive composites could be formed: a thermal gate wherein all flow was blocked through the column or a thermal valve which can control flow rate. With the expansion and contraction of the polymer at different temperatures, the resulting change in functionality could be exploited. By controlling temperature, the thermal responsive polymer could be used to selectively elute hydrophilic analytes at high temperatures and to elute hydrophobic analytes at a lower temperature. Viklund *et al.* grafted the charged monomer AMPS, to an otherwise neutral poly(GMA-*co*-EDMA) monolithic column [94]. The polymerization was terminated by cooling the column and extensive washing. The column was used for the separation of proteins (myoglobin, chymotrypsinogen, lysozyme) with an efficiency of 6,700 N/m for lysozyme.

Poly(trimethylolpropane trimethacrylate) (poly(TRIM)) monoliths were thermally grafted with the zwitterionic monomer MEDSA [95], which retained basic proteins when loaded from pure water.

Other thermally initiated polymerizations used in post-polymerization modification have been employed to introduce new surface functionality and to improve the fine control of porous properties in polymer monolithic columns. A polymerization that can restart chain growth upon the addition of a new monomer is called "living". During the polymerization process the stable free radicals are combined with the growing polymer chains. A functional monomer can then be added to the structure, and with the activation of latent dormant radicals, surface localized grafting can proceed upon the application of temperature [96]. This may provide a method for controlling the phase separation, resulting in a more homogeneous monolithic column [17].

There are numerous types of living polymerization approaches such as nitroxide mediated polymerization [96,97], ring opening metathesis polymerization (ROMP) [98,99], atom transfer radical polymerization (ATRP) [100,101], and reversible addition-fragmentation chain transfer polymerization (RAFT) [102,103]. Some of these methods have been used in the fabrication of cross-linked gels [100], polymer beads [101], and polymer monoliths [96,104]. Temperatures above 100 °C are generally used, while termination of the growing polymer is mediated by decreasing the temperature [104]. Peters *et al*. used 2,2,6,6-tetramethylpiperidyl-1-oxy (TEMPO) facilitated polymerizations for the subsequent grafting of the resulting polymer [105]. Either HEMA or VBC were grafted to the column in the presence of initiators such as benzoyl peroxide (BPO) and TEMPO.

Meyer *et al*. prepared poly(STY-*co*-DVB) monolithic columns [96]. Using a simplified grafting reaction, wherein the monomer and solvent (cyclohexanol) were only present in the column, the surface latent initiators facilitated the reaction. The graft polymerization proceeded at an elevated temperature of 110 °C. Viklund *et al*. prepared poly(STY-*co*-DVB) monolithic columns using BPO and a stable free radical [104]. The hydrophobic poly(STY-*co*-DVB) column was grafted with a hydrophilic monomer (HEMA) using the latent surface radicals. SPM was also grafted to the column using a solution of monomer in dimethyl sulfoxide. The hyrdophilized column (HEMA graft) showed a significantly reduced retention and a decrease in pore volume of 11.5% following grafting. The SPM grafted monolith was used in the cation exchange of proteins, namely myoglobin, cytochrome c, and lysozyme.
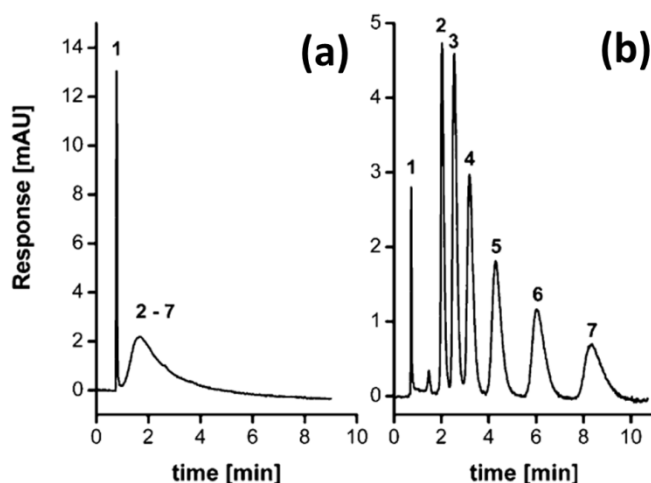
5. Hypercross-Linking

A pre-cursor material or substrate is solvated in a thermodynamically good solvent, where a cross-linking reaction locks the polymer chains in a state similar to that in the solvated state [106]. Following the removal of the solvent, the remaining structures are the new pores within the material, adding significantly to surface area in polymer monolithic columns. The origins of hypercross-linking are connected with Davankov *et al*. from the 1970's to the early 2000's [107–111]. Generic monolithic columns with relatively low specific surface area (usually <10 m^2/g [2]) can be improved upon by a straightforward post-polymerization modification, the hypercross-linking method.

Urban *et al*. highlighted the main theoretical considerations of hypercross-linking by Friedel-Crafts reaction [112]. The extent of DVB in the monomer precursor and the ratio to vinyl benzyl chloride (VBC) controls the degree of cross-linking, as well as the ratio of VBC to STY, which controls the

distance between reactive chloromethyl sites and the extent of hypercross-linking. Hypercross-linking was performed in monolithic columns, using poly(STY-*co*-VBC-*co*-DVB) monolithic columns [112]. The porosity of the monolith was not altered due to the minimal mass of the cross-linked moieties, however, the surface area of the monolith was increased from 29 m^2/g to 663 m^2/g, which is twice that of silica monolithic columns [113].

The isocratic separation of small molecules before modification showed little efficiency. Following the cross-linking reaction, the separation efficiency for alkylbenzenes performed under the same conditions (see Figure 5), was increased to 73,000 N/m. In the gradient separation of proteins, however, the efficiency was significantly reduced, as the introduction of meso-pores resulted in the higher impedance of mass transfer of the proteins. The group investigated the effects of the reaction conditions (temperature, time) upon the cross-linking [114]. The surface area increased dramatically for reaction times of up to 2 h, however, no significant changes in surface area were obtained at greater reaction times. The column was successfully used in three separation types: small molecules (alkylbenzenes), biomolecules (a tryptic digest of the cytochrome c protein), and size exclusion (toluene with polystyrene standards of varying molecular size). A column temperature of 80 °C produced columns with the best efficiencies and lower resistance to mass transfer when compared to lower column temperatures. Separations performed with the column hypercross-linked at 90 °C for 2 h, produced plate heights in excess of 80,000 N/m.

Figure 5. Separation of uracil and alkylbenzenes using a (**a**) generic precursor poly(STY-*co*-VBC-*co*-DVB) monolithic column, and (**b**) the hypercross-linked counterpart. Separation conditions were 80% ACN, a flow rate of 1.5 µL/min, and UV detection at 254 nm. Peaks: uracil (1), benzene (2), toluene (3), ethylbenzene (4), propylbenzene (5), butylbenzene (6), and amylbenzene (7). Reprinted with permission. Adapted with permission from [112]. Copyright (2010) American Chemical Society.

Using the procedure outlined by Urban *et al*. [114], Chen *et al*. produced hypercross-linked columns for applications in CEC [115]. Poly(STY-*co*-DVB-*co*-VBC) and poly(MST-*co*-DVB-*co*-VBC) columns were prepared and hypercross-linked. The hypercross-linked poly(STY-*co*-DVB-*co*-VBC) demonstrated a 34-fold increase in EOF, while the hypercross-linked poly(MST-*co*-DVB-*co*-VBC) exhibited a 21 fold increase, relative to the unmodified generic monolith. The increase in EOF was

attributed to the increase in surface area in the column due to the formation of new meso-pores. Another use of the column design by Urban *et al*. [114] was demonstrated by Teisseyre *et al*. who coupled NMR to on-line micro-HPLC separations [116].

The technique of hypercross-linking has recently been extended by Škeřiková *et al*., wherein following hypercross-linking, a monomer (MEDSA) was thermally grafted to the resulting porous structure [117]. Using IR characterization, the presence of MEDSA was detected in modified columns. The surface modification demonstrated an excellent stability, with a % RSD no greater than 4%, for retention times following 500 injections. The modified column demonstrated a dual retention mechanism, dependent on the amount of water in the mobile phase (φ H_2O), characteristic of such HILIC columns [30–35]. Hypercross-linking may be combined for further modification, for example, with nano-particles, for the preparation of novel stationary phases [118]. A comparison of hypercross-linking reactions can be seen in Table 3.

Table 3. Hypercross-linking used in the preparation of enhanced surface area polymeric monolithic columns.

Monolith	Reaction	Temperature (°C)	Time (h)	Reference
Poly(styrene-*co*-VBC-*co*-DVB)	Solution of FeCl$_3$ in DCE flushed across column (held in ice for 2 h).	80	24	[112]
Poly(styrene-*co*-VBC-*co*-DVB)	Solution of FeCl$_3$ in DCE flushed across column (held in ice for 1 h).	80	24	[114]
Poly(styrene-*co*-VBC-*co*-DVB) and poly(4-methyl styrene -*co*-VBC-*co*-DVB)	Solution of FeCl$_3$ in DCE flushed across column (held in ice for 2 h).	90	2	[115]
Poly(styrene-*co*-VBC-*co*-DVB)	Solution of FeCl$_3$ in DCE flushed across column.	90	2	[116]
Poly(styrene-*co*-VBC-*co*-DVB)	Solution of FeCl$_3$ in DCE flushed across column. Thermal grafting of MEDSA using 4,4'-azobis(4-cyanovaleric acid) (8 h at 70 °C).	90	2	[117]
Poly(4-methyl styrene -*co*-VBC-*co*-DVB)	Hypercross-linked monolith brominated to support cysteamine modification (microwave assisted, 30 min). Disulphide bonds cleaved. Pendent thiols modified with AuNPs.	90	4	[118]

6. Nano-Particles and Nano-Structures

Nano-particles are characterized by their high volume to surface area ratio [119], and as such can also be used to increase the surface area of polymeric monolithic columns *in situ*. Nano-architectures can also be used to introduce additional surface functionality to polymeric monolithic columns [9,118–141]. Nano-particles and nano-structures can be introduced to monolithic columns primarily through two routes: firstly, the addition of the nano-particle or nano-structure to the monolith precursor solution prior to monolith polymerization (encapsulation) [120–128], or secondly, by immobilization on the monolith surface [9,129–139]. Three excellent reviews on nano-particle modifications have been recently published, dealing with both nano-particle modified stationary

phases for biomolecule immobilizations, such as extraction applications [27] and nano-particle stationary phases for columns in HPLC separations [140,141], and tissue engineering [140]. Each method of modification has its own merits, however, as with co-polymerization of functional monomers, the monolith structure can be changed by varying any one parameter of the precursor mixture, which can be detrimental in the finite control of column morphology. The current review is limited to post-polymerization modifications, and so encapsulation (co-polymerization) will not be discussed further. In surface modification with nano-materials, wherein a functional group responsible for nano-particle attachment is co-polymerized into the monolith, again the surface coverage may be low, thus limiting the effect of nano-particle or nano-structure addition. A summary of surface modifications using nano-materials can be seen in Table 4.

Table 4. Reactions used in the preparation of nano-agglomerated polymeric monoliths.

Monolith	Reaction	Temperature (C°)	Time	Nano-Particle Type	Reference
Poly(BuMA-*co*-EDMA) and poly(LMA-*co*-EDMA)	Introduction of photo-grafted zones of monomers suitable for amination, supporting AuNP immobilization. Dual function monolith.	Room Temperature (RT)	N/A	20 nm Au	[9]
Poly(GMA-*co*-EDMA) and poly(styrene-*co*-DVB)	For poly(STY-*co*-DVB) chlorosulfonic acid in dry dichloromethane was used for sulfonation. For poly(GMA-*co*-EDMA), sulfonation was performed in three techniques: (i) 4-hydroxybenezenesulfonic acid and triethylamine, (ii) thiobenzoic acid and triethylamine (thiol groups were oxidized by pumping a solution of tert-butylhydroperoxide). (iii) Sodium sulfite and tetra-n-butylammonium hydroxide.	60, 60, 70, respectively	20 h each	65 nm Latex	[28]
Poly(BuMA-*co*-AMPS-*co*-EDMA)	Co-polymerization of sulfonic acid group suitable for latex nano-particle agglomeration.	RT	2 h	60 nm Latex	[46]
Poly(BuMA-*co*-AMPS-*co*-EDMA)	Co-polymerization of sulfonic acid group suitable for latex nano-particle agglomeration.	RT	2 h	65 nm Latex	[47]
Poly(BuMA-*co*-AMPS-*co*-EDMA)	Co-polymerization of sulfonic acid group suitable for latex nano-particle agglomeration.	RT	2 h	65 nm Latex	[48]
Poly(GMA-*co*-EDMA)	Introduction of surface immobilized AuNPs via cysteamine and subsequent cleavage of the disulfide bond, to reveal surface thiols. AuNP modification.	RT	N/A	10 nm Au	[118]
Poly(GMA-co-EDMA)	Generation of quaternary ammonium for IONP immobilization.	RT	N/A	19 nm iron oxide	[119]
Poly(EDMA)	Preparation of AuNP modified extraction pipette tip, for glycoprotein selectivity.	RT	N/A	20 nm Au	[129]
Poly(GMA-*co*-EDMA)	Coupling of α-glucosidase to AuNP modified monolith for PMME.	RT	3 h	15 nm Au	[130]
Poly(GMA-*co*-EDMA)	For AuNP immobilization, and functionalizing groups such as 3-mercapto propionic acid (CEC), 1-octadecanethiol (RPLC), and sodium 2-mercaptoethane sulfonate (SCX).	RT	N/A	15 nm Au	[131]

Table 4. *Cont.*

Monolith	Reaction	Temperature (C°)	Time	Nano-Particle Type	Reference
Poly(NAS-*co*-EDMA)	Surface generation of alkyne group, followed by thiol-yne photo-addition of cysteamine for AuNP modification.	RT	N/A	20 nm Au	[132]
Poly(GMA-*co*-EDMA)	Introduction of surface AuNPs by generation of surface thiols from surface epoxide groups. Two methods were used: (i) Hydrogen sulfide, and (ii) Cysteamine.	100 RT RT	30 min 2 h 20 min	40–50 nm Au	[133]
Poly(BuMA-*co*-EDMA)	Preparation of thiolated and aminated surfaces and comparison of immobilization pathways for AuNPs.	RT	N/A	20 nm Au	[134]
Poly(GMA-*co*-EDMA)	Immobilization of SNPs upon a polymer monolith.	RT	60 min	50 nm Ag	[127]
Poly(HEMA-*co*-EDMA)	Generation of polymer monolith extraction device within a pipette tip, immobilized with IONPs via surface grafted functional groups (META).	RT	N/A	20 nm iron oxide	[135]
Poly(NIPAAm-*co*-GMA-*co*-EDMA)	Generation of γ-alumina nano-particle monolith for PMME.	60	14 h	10–20 nm Al$_2$O$_3$	[136]
Poly(GMA-*co*-EDMA), poly(BuMA-*co*-EDMA), poly(GMA-*co*-BuMA-*co*-EDMA)	Immobilization of Pd/Pt NFs via aminated surface groups.	RT	72 h	Pd/Pt NFs	[137]
Poly(GMA-*co*-EDMA)	Coating of monolith surface with graphene and graphene oxide nano-sheets for PMME.	RT	N/A	Graphene nano-sheets	[138]
Poly(GMA-*co*-EDMA)	Encapsulation of MWCNTs and surface attachment of MWCNTs via surface aminated groups.	RT	N/A	MWCNTs	[139]

6.1. Polymeric Nano-Particles

The use of quaternary amine-functionalized latex nano-particles was reported by Hilder *et al*. [46], and later by Hutchinson *et al*. [28,47,48]. The generic monoliths were prepared using a single step polymerization, incorporating AMPS into the monolith matrix. The anion exchange nano-particles (60 nm diameter) were flushed across the column to facilitate coating, via coloumbic interactions. One of the advantages was the increase in surface area, which improved by approximately 30% relative to the unmodified column. This column type has been used successfully in the separation of carbohydrates [46], inorganic ions in sea water, and in mili Q water [48].

6.2. Gold Nano-Particles

The immobilization of nano-particles has been used to improve the surface area of polymeric monolithic columns [119], to facilitate the addition of a functional group [129,130], and to provide a substrate to facilitate interchangeable surface chemistry [131]. In addition to the use of gold nano-particles (AuNPs), the methods used in the immobilization procedures vary from latent reactive surface groups, such as those generated by co-polymerization of reactive monomers (e.g., GMA, NAS) [132], and the grafting of functional groups capable of supporting aminated or thiolated groups for immobilization of AuNPs [9,129–131]. A method for the preparation of AuNPs was described by Frens *et al*. in the 1970's, in which the concentration of reducing agent controlled the resulting

nano-particle diameter [142]. Generally, the AuNPs are formed *in vitro* prior to addition to a preformed monolithic column [9,129,134]. Alternative methods can also be used, such as the mixing of the AuNP suspension with a reducing agent directly before entering the column, *i.e.*, by use of a T-piece [131,133].

In numerous studies [9,129,134], the reactive monomers VAL or GMA were grafted to monoliths, in order to produce the typical surface for AuNP immobilization. Aminated and thiolated surfaces for AuNP immobilization were investigated; amination provided uniformly spaced nano-particles, whereas a thiolated surface produced sporadic aggregates of nano-particle clusters [134]. The aminated pathway generated a higher gold wt% content on the monolith surface relative to previously reported thiolated methods [131,133]. Lv *et al.* produced a hypercross-linked column, which incorporated the use of both surface thiol groups and a secondary immobilization of amine groups (polyethyleneimine, PEI) [118]. The thiol layer was responsible for the primary loading of 20 nm AuNPs whilst the secondary PEI layer supported the immobilization of 10 nm AuNPs. Ultimately, the column demonstrated both an increase in available surface area and an increase in separation efficiency. As the total content of gold was lower than in previously reported columns [131,134], this increase in efficiency may have been due to the hypercross-linking step alone. Once the AuNPs have been immobilized, the surface can be used for additional functionalization. For example, Cao *et al.* have used the AuNP surface to produce switchable surface chemistries [131]. By exploiting the interaction between thiols and gold, a number of molecules were used to produce RPLC functionality, ion exchange functionality, and charged groups for CEC separations. Each stationary phase demonstrated the separation ability and the stability of the AuNP coating, using model analytes of three proteins: ribonuclease A, cyctochrome C, and myoglobin. This method of coating is also temperature sensitive, as described by Xu *et al.* [133], wherein the AuNP surface can be regenerated using temperatures of above 80 °C and water to remove thiols. An example of immobilized AuNPs upon a polymer monolith is shown in Figure 6.

Figure 6. FE-SEM micrograph of a poly(LMA-*co*-EDMA) monolith with aminated poly(GMA) grafted chains to support AuNP immobilization. Reprinted from [9]. Copyright (2013), with permission from Elsevier.
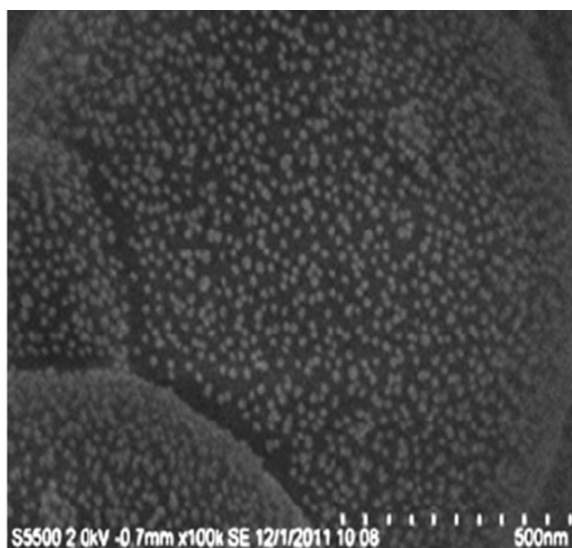
Immobilized AuNPs can also be utilized in the preparation of affinity phases. Alwael *et al.* produced poly(EDMA) monoliths within the confines of polypropylene pipette tips, which were subsequently modified with AuNPs [129]. The monolith ultimately expressed a lectin, which could be selectively used to extract glycoproteins from complex mixtures. The pipette tip demonstrated an extraction efficiency of up to 37% and a recovery efficiency of 86% to 100%. A segmented AuNP monolith was produced by Currivan *et al.* [9], wherein, similar to the photo-grafting work performed by Logan *et al.* [8], a column expressing two discreet zones was prepared. A section of column dedicated to AuNP immobilization was followed by a RP zone, and using an elution technique [133], cysteine containing peptides could be extracted and separated, within a single column. In addition, Zhang *et al.* produced an AuNP modified monolithic enzymatic microreactor within a capillary for CE [130]. The AuNPs were modified with α-glucosidase and used in the screening of α-glucosidase inhibitors in a range of natural products.

6.3. Other Metallic Nano-Particles

The use of AuNPs has become extremely popular in recent years, however, other metallic nano-particles are also available. Monoliths with metallic or metal oxide nano-particles such as nickel-cobalt [124] and titanium dioxide [125,126], have been prepared via encapsulation (co-polymerization) techniques. In contrast, using a hydrophilic monolithic column (poly(GMA-*co*-trimethylolpropane triacrylate)), silver nanoparticles (SNPs) were trapped in the crevices of the monolithic column. The SNP modified column was effectively used as a detection element for surface enhanced Raman spectroscopy (SERS) [127]. Iron oxide nano-particles (IONPs) have also been used to prepare monolithic media in both column [119] and pipette format [135]. Křenková *et al.* prepared poly(GMA-*co*-EDMA) monolithic columns for modification with IONPs [119]. The IONP modified column was applied to the enrichment of phosphopeptides (α-casein, and β-casein tryptic digests) with MS detection. When compared to commercially available TiO_2 pipette tips, the monolithic column demonstrated greater selectivity. Using ATP, the binding capacity of the monolith was found to be 47.4 mg/mL column volume (86 μmol/mL column volume). The group later extended this technology to the confines of a pipette tip [135]. The quaternary ammonium monomer META was grafted to the monolith, enabling the immobilization of IONPs. The pipette tip was used in the enrichment of phosphopeptides (α-casein, and β-casein) and was compared to commercially available TiO_2 tips, and again the IONP modified monolithic tip exhibited superior selectivity.

Using a poly(N-isopropylacrylamide-*co*-GMA-*co*-EDMA) monolith, Li *et al.* immobilized γ-Al_2O_3 nano-particles [136]. The material was used in the polymer monolith micro-extraction (PMME) procedure of Sudan dyes in red wine samples. Using a subsequent HPLC method (particle packed C_{18} column) the dye extract was detected, and the extraction efficiency ranged from 84% to 116%. The nano-particle modified monolith was compared to a polymer only column and to direct HPLC analysis of the wine samples for each dye (Sudan I-IV). A four-fold increase in peak area for the nano-particle modified column relative to the polymer monolith alone and an eight-fold increase relative to direct HPLC analysis were demonstrated. Nano-particles consisting of a composite of metals have also been immobilized to preformed poly(BuMA-*co*-EDMA) columns grafted with VAL or GMA [137]. Floris *et al.* produced nano-flower (NF) immobilized columns [137]. Platinum/palladium NFs consist of a platinum

core to which palladium "petals" were immobilized. Following column amination, the NFs were immobilized to the monolith surface. The columns were evaluated using chromatography via anion exchange, performed before and following modification. The NF modified column was also successful in catalysis, in the catalytic reduction of Fe(III) to Fe (II), and the catalytic oxidation of NADH to NAD$^+$. The immobilized NFs demonstrated excellent reproducibility and stability in the presence of strong reducing agents such as sodium borohydride.

6.4. Carbon Nano-Structures

Nano-structures have also been used in the preparation of monolithic columns and encompass carbon nano-structures (e.g., multi-walled carbon nano-tubes, MWCNTs), graphene, and nano-diamonds [138–141].

Chambers *et al*. described both the encapsulation method and surface modification with MWCNTs [139]. They prepared poly(GMA-*co*-EDMA) monolithic columns, which were treated with ammonium hydroxide, resulting in an amine expressing surface. The MWCNTs were subjected to a cutting procedure, which resulted in the generation of carboxylic acids at the end of the tube wall. This renders the tubes slightly hydrophilic, however, sufficient hydrophobicity is maintained. The unmodified column demonstrated no separation of any alkylbenzene analytes, whilst following modification, all seven peaks in the sample mixture were resolved (benzene, toluene, ethylbenzene, propylbenzene, butylbenzene, and amylbenzene) with an efficiency of 23,000 N/m obtained for benzene. The separation was improved by reducing the average pore size (thus increasing the surface area), however, a three-fold increase in pressure drop across the column was also obtained. The increase in surface area also resulted in an increase in MWCNT coverage, thus accounting for the increased efficiency (40,000 N/m for benzene).

7. Concluding Remarks

The use of post-polymerization modification has been shown to increase the efficiency of surface coverage of functional groups relative to co-polymerization methods. A wide variety of surface modification reactions are available for free radical initiated polymer monolithic columns, with a larger arsenal if living polymerizations are also considered. Photo-grafting techniques are extremely useful in the fine control of surface chemistry, both in functionality and spatial location, particularly with consideration of microfluidic devices, which encompass monolithic media. Enzymatic reactors have been prepared in monolithic media many times, each with their specific applications. However, the importance of hydrophilization of the support material has also been discussed. From earlier applications of co-polymerization, photo-grafting techniques have since dominated with great success. The inherent difficulties of surface area in polymer monoliths, with small molecule applications have also been addressed by post-polymerization modifications. Hypercross-linking has proven to be a technically straightforward technique in providing "pseudo meso-pores" in polymeric media and has shown recent progress with additional surface grafting. This can result in the next generation of high capacity separation polymeric monolithic columns. In addition, inherently high surface to volume ratio nano-particles have also been integrated into such high surface area materials, and to reduced surface area materials, again with the incentive to create high capacity materials for separations. The further

modification of nano-material expressing materials to other chemistries has also demonstrated the potential of future monolithic column modifications, and thus, applications.

Acknowledgments

Conflicts of Interest

The authors declare no conflict of interest.

References

1. Hjertén, S.; Liao, J.; Zhang, R. High-performance liquid chromatography on continuous polymer beds. *J. Chromatogr.* **1989**, *473*, 273–275.
2. Svec, F.; Fréchet, J. Continuous rods of macroporous polymer as high-performance liquid chromatography separation media. *Anal. Chem.* **1992**, *64*, 820–822.
3. Svec, F.; Fréchet, J. Modified poly(glycidyl methacrylate-co-ethylene dimethacrylate) continuous rod columns for preparative-scale ion-exchange chromatography of proteins. *J. Chromatogr. A* **1995**, *702*, 89–95.
4. Peters, E.; Petro, M.; Svec, F.; Fréchet, J. Molded rigid polymer monoliths as separation media for capillary electrochromatography. *Anal. Chem.* **1997**, *69*, 3646–3649.
5. Xie, S.; Svec, F.; Fréchet, J. Design of reactive porous polymer supports for high throughput bioreactors: Poly(2-vinyl-4,4-dimethylazlactone-co-acrylamide-co-ethylene dimethacrylate) monoliths. *Biotechnol. Bioeng.* **1999**, *62*, 30–35.
6. Peterson, D.; Rohr, T.; Svec, F.; Fréchet, J. Enzymatic microreactor-on-a-chip: Protein mapping using trypsin immobilized on porous polymer monoliths molded in channels of microfluidic devices. *Anal. Chem.* **2002**, *74*, 4081–4088.
7. Stachowiak, T.; Svec, F.; Fréchet, J. Patternable protein resistant surfaces for multifunctional microfluidic devices via surface hydrophilization of porous polymer monoliths using photografting. *Chem. Mater.* **2006**, *18*, 5950–5957.
8. Logan, T.; Clarke, D.; Stachowiak, T.; Svec, F.; Fréchet, J. Photopatterning enzymes on polymer monoliths in microfluidic devices for steady-state kinetic analysis and spatially separated multi-enzyme reactions. *Anal. Chem.* **2007**, *79*, 6592–6598.
9. Currivan, S.; Connolly, D.; Paull, B. Production of polymer monolithic capillary columns with integrated gold nano-particle modified segments for on-capillary extraction. *Microchem. J.* **2013**, *111*, 32–39.
10. Pucci, V.; Raggi, M.; Svec, F.; Fréchet, J. Monolithic columns with a gradient of functionalities prepared via photoinitiated grafting for separations using capillary electrochromatography. *J. Sep. Sci.* **2004**, *27*, 779–788.

11. Currivan, S.; Connolly, D.; Gillespie, E.; Paull, B. Fabrication and characterisation of capillary polymeric monoliths incorporating continuous stationary phase gradients. *J. Sep. Sci.* **2010**, *33*, 484–492.

12. Collins, D.; Nesterenko, E.; Connolly, D.; Vasquez, M.; Macka, M.; Brabazon, D.; Paull, B. Versatile capillary column temperature control using a thermoelectric array based platform. *Anal. Chem.* **2011**, *83*, 4307–4313.

13. Currivan, S.; Connolly, D.; Paull, B. Production of novel polymer monolithic columns, with stationary phase gradients, using cyclic olefin co-polymer (COC) optical filters. *Analyst* **2012**, *137*, 2559–2566.

14. Peters, E.; Svec, F.; Fréchet, J. Rigid macroporous polymer monoliths. *Adv. Mater.* **1999**, *11*, 1169–1181.

15. Svec, F.; Fréchet, J. Molded rigid monolithic porous polymers: An inexpensive, efficient, and versatile alternative to beads for the design of materials for numerous applications. *Ind. Eng. Chem. Res.* **1999**, *38*, 34–48.

16. Svec, F. Preparation and HPLC applications of rigid macroporous organic polymer monoliths. *J. Sep. Sci.* **2004**, *27*, 747–766.

17. Svec F. Porous polymer monoliths: Amazingly wide variety of techniques enabling their preparation. *J. Chromatogr. A* **2010**, *1217*, 902–924.

18. Svec, F. Quest for organic polymer-based monolithic columns affording enhanced efficiency in high performance liquid chromatography separations of small molecules in isocratic mode. *J. Chromatogr. A* **2012**, *1228*, 250–262.

19. Schaller, D.; Hilder, E.; Haddad, P. Monolithic stationary phases for fast ion chromatography and capillary electrochromatography of inorganic ions. *J. Sep. Sci.* **2006**, *29*, 1705–1719.

20. Nordborg, A.; Hilder, E. Recent advances in polymer monoliths for ion-exchange chromatography. *Anal. Bioanal. Chem.* **2009**, *394*, 71–84.

21. Svec, F. Less common applications of monoliths: I. Microscale protein mapping with proteolytic enzymes immobilized on monolithic supports. *Electrophoresis* **2006**, *27*, 947–961.

22. Svec, F. Less common applications of monoliths: Preconcentration and solid-phase extraction. *J. Chromatogr. B* **2006**, *841*, 52–64.

23. Potter, O.; Hilder, E. Porous polymer monoliths for extraction: Diverse applications and platforms. *J. Sep. Sci.* **2008**, *31*, 1881–1906.

24. Mallik, R.; Hage, D. Affinity monolith chromatography. *J. Sep. Sci.* **2006**, *29*, 1686–1704.

25. Arrua, R.; Alvarez-Igarzabal, C. Macroporous monolithic supports for affinity chromatography. *J. Sep. Sci.* **2011**, *34*, 1974–1987.

26. Calleri, E.; Ambrosini, S.; Temporini, C.; Massolini, G. New monolithic chromatographic supports for macromolecules immobilization: Challenges and opportunities. *J. Pharm. Biomed. Anal.* **2012**, *69*, 64–76.

27. Connolly, D.; Currivan, S.; Paull, B. Polymeric monolithic materials modified with nanoparticles for separation and detection of biomolecules: A review. *Proteomics* **2012**, *12*, 2904–2917.

28. Hutchinson, J.; Hilder, E.; Shellie, R.; Smith, J.; Haddad, P. Towards high capacity latex-coated porous polymer monoliths as ion-exchange stationary phases. *Analyst* **2006**, *131*, 215–221.

29. Gillespie, E.; Connolly, D.; Paull, B. Using scanning contactless conductivity to optimise photografting procedures and capacity in the production of polymer ion-exchange monoliths. *Analyst* **2009**, *134*, 1314–1321.

30. Jiang, Z.; Smith, N.; Ferguson, P.; Taylor, M. Hydrophilic interaction chromatography using methacrylate-based monolithic capillary column for the separation of polar analytes. *Anal. Chem.* **2007**, *79*, 1243–1250.

31. Jiang, Z.; Reilly, J.; Everatt, B.; Smith, N. Novel zwitterionic polyphosphorylcholine monolithic column for hydrophilic interaction chromatography. *J. Chromatogr. A* **2009**, *1216*, 2439–2448.

32. Jiang, Z.; Smith, N.; Ferguson, P.; Taylor, M. Novel highly hydrophilic zwitterionic monolithic column for hydrophilic interaction chromatography. *J. Sep. Sci.* **2009**, *32*, 2544–2555.

33. Jandera, P.; Staňková, M.; Škeříková, V.; Urban, J. Cross-linker effects on the separation efficiency on (poly)methacrylate capillary monolithic columns. Part I. Reversed-phase liquid chromatography. *J. Chromatogr. A* **2013**, *1274*, 97–106.

34. Staňková, M.; Jandera, P.; Škeříková, V.; Urban, J. Cross-linker effects on the separation efficiency on (poly)methacrylate capillary monolithic columns. Part II. Aqueous normal-phase liquid chromatography. *J. Chromatogr. A* **2013**, *1289*, 47–57.

35. Liu, Z.; Peng, Y.; Wang, T.; Yuan, G.; Zhang, Q.; Guo, J.; Jiang, Z. Preparation and application of novel zwitterionic monolithic column for hydrophilic interaction chromatography. *J. Sep. Sci.* **2013**, *36*, 262–269.

36. Hilder, E.; Svec, F.; Fréchet, J. Shielded stationary phases based on porous polymer monoliths for the capillary electrochromatography of highly basic biomolecules. *Anal. Chem.* **2004**, *76*, 3887–3892.

37. Rohr, T.; Hilder, E.; Donovan, J.; Svec, F.; Fréchet, J. Photografting and the control of surface chemistry in three-dimensional porous polymer monoliths. *Macromolecules* **2003**, *36*, 1677–1684.

38. Peters, E.; Svec, F.; Fréchet, J. Thermally responsive rigid polymer monoliths. *Adv. Mater.* **1997**, *9*, 630–633.

39. Chen, H.; Huang, T.; Zhang, X. Immunoaffinity extraction of testosterone by antibody immobilized monolithic capillary with on-line laser-induced fluorescence detection. *Talanta* **2009**, *78*, 259–264.

40. Guerrouache, M.; Millot, M.; Carbonnier, B. Functionalization of macroporous organic polymer monolith based on succinimide ester reactivity for chiral capillary chromatography: A cyclodextrin click approach. *Macromol. Rapid Commun.* **2009**, *30*, 109–113.

41. Palm, A.; Novotny, M. A monolithic PNGase F enzyme microreactor enabling glycan mass mapping of glycoproteins by mass spectrometry. *Rapid Commun. Mass Spectrom.* **2005**, *19*, 1730–1738.

42. Guerrouche, M.; Millot, M.; Carbonnier, B. Capillary columns for reversed-phase CEC prepared via surface functionalization of polymer monolith with aromatic selectors. *J. Sep. Sci.* **2011**, *34*, 2271–2278.

43. Dao, T.; Guerrouche, M.; Carbonnier, B. Thiol-yne click adamantane monolithic stationary phase for capillary electrochromatography. *Chin. J. Chem.* **2012**, *30*, 2281–2284.

44. Sýkora, D.; Svec, F.; Fréchet, J. Separation of oligonucleotides on novel monolithic columns with ion-exchange functional surfaces. *J. Chromatogr. A* **1999**, *852*, 297–304.

45. Ueki, Y.; Umemura, T.; Li, J.; Odake, T.; Tsunoda, K. Preparation and application of methacrylate-based cation-exchange monolithic columns for capillary ion chromatography. *Anal. Chem.* **2004**, *76*, 7007–7012.

46. Hilder, E.; Svec, F.; Fréchet, J. Latex-functionalized monolithic columns for the separation of carbohydrates by micro anion-exchange chromatography. *J. Chromatogr. A* **2004**, *1053*, 101–106.

47. Hutchinson, J.; Zakaria, P.; Bowie, A.; Macka, M.; Avdalovic, N.; Haddad, P. Latex-coated polymeric monolithic ion-exchange stationary phases. 1. Anion-exchange capillary electrochromatography and in-line sample preconcentration in capillary electrophoresis. *Anal. Chem.* **2005**, *77*, 407–416.

48. Zakaria, P.; Hutchinson, J.; Avdalovic, N.; Liu, Y.; Haddad, P. Latex-coated polymeric monolithic ion-exchange stationary phases. Micro-ion chromatography. *Anal. Chem.* **2005**, *77*, 417–423.

49. Bisjak, C.; Bakry, R.; Huck, C.; Bonn, G. Amino-functionalized monolithic poly(glycidyl methacrylate-co-divinylbenzene) ion-exchange stationary phases for the separation of oligonucleotides. *Chromatographia* **2005**, *62*, S31–S36.

50. Preinerstorfer, B.; Linder, W.; Lämmerhofer, M. Polymethacrylate-type monoliths functionalized with chiral amino phosphonic acid-derived strong cation exchange moieties for enantioselective nonaqueous capillary electrochromatography and investigation of the chemical composition of the monolithic polymer. *Electrophoresis* **2005**, *26*, 2005–2018.

51. Weider, W.; Bisjak, C.; Huck, C.; Bakry, R.; Bonn, G. Monolithic poly(glycidyl methacrylate-co-divinylbenzene) capillary columns functionalized to strong anion exchangers for nucleotide and oligonucleotide separation. *J. Sep. Sci.* **2006**, *29*, 2478–2484.

52. Lou, Q.; Zou, H.; Xiao, X.; Gou, Z.; Kong, L.; Mao, X. Chromatographic separation of proteins on metal immobilized iminodiacetic acid-bound molded monolithic rods of macroporous poly(glycidyl methacrylate-co-ethylene dimethacrylate). *J. Chromatogr. A* **2001**, *926*, 255–264.

53. Pan, Z.; Zou, H.; Mo, W.; Huang, X.; Wu, R. Protein A immobilized monolithic capillary column for affinity chromatography. *Anal. Chim. Acta* **2002**, *466*, 141–150.

54. Bedair, M.; El Rassi, Z. Affinity chromatography with monolithic capillary columns I. Polymethacrylate monoliths with immobilized mannan for the separation of mannose-binding proteins by capillary electrochromatography and nano-scale liquid chromatography. *J. Chromatogr. A* **2004**, *1044*, 177–186.

55. Bedair, M.; El Rassi, Z. Affinity chromatography with monolithic capillary columns II. Polymethacrylate monoliths with immobilized lectins for the separation of glycoconjugates by nano-liquid affinity chromatography. *J. Chromatogr. A* **2005**, *1079*, 236–245.

56. Bedair, M.; Oleschuk, R. Lectin affinity chromatography using porous polymer monolith assisted nanoelectrospray MS/MS. *Analyst* **2006**, *131*, 1316–1321.

57. Yang, C.; Zhu, G.; Zhang, L.; Zhang, W.; Zhang, Y. Repeatedly usable immobilized pH gradient in a monolithic capillary column. *Electrophoresis* **2004**, *25*, 1729–1734.

58. Zhu, G.; Yuan, H.; Zhao, P.; Zhang, L.; Liang, Z.; Zhang, W.; Zhang, Y.; Macroporous polyacrylamide-based monolithic column with immobilized pH gradient for protein analysis. *Electrophoresis* **2006**, *27*, 3578–3583.

59. Liang, Y.; Zhu, G.; Wang, T.; Zhang, X.; Liang, Z.; Zhang, L.; Zhang, Y. Fast preparation of monolithic immobilized pH gradient column by photopolymerization and photografting techniques for isoelectric focusing separation of proteins. *Electrophoresis* **2011**, *32*, 2911–2914.

60. Rånby, B. Photochemical modification of polymers-photocrosslinking, surface photografting, and lamination. *Polym. Eng. Sci.* **1998**, *38*, 1229–1243.

61. Rånby, B.; Yang, W.; Tretinnikov, O. Surface photografting of polymer fibers, films and sheets. *Nucl. Instrum. Methods Phys. Res. B* **1999**, *151*, 301–305.

62. Rånby, B. Surface modification and lamination of polymers by photografting. *Int. J. Adhes. Adhes.* **1999**, *19*, 337–343.

63. Rånby, B. Photoinitiated modifications of polymers: Photocrosslinking, surface photografting and photolamination. *Mater. Res. Innov.* **1998**, *2*, 64–71.

64. Yang, W.; Rånby, B. Bulk surface photografting process and its applications. I. Reactions and kinetics. *J. App. Polym. Sci.* **1996**, *62*, 533–543.

65. Yang, W.; Rånby, B. Photoinitiation performance of some ketones in the LDPE-acrylic acid surface photografting system. *Eur. Polym. J.* **1999**, *35*, 1557–1568.

66. Viklund, C.; Ponten, E.; Glad, B.; Irgum, K.; Horstedt, P.; Svec, F. "Molded" macroporous poly(glycidyl methacrylate-co-trimethylolpropane trimethacrylate) materials with fine controlled porous properties: Preparation of monoliths using photoinitiated polymerization. *Chem. Mater.* **1997**, *9*, 463–471.

67. Eeltink, S.; Hilder, E.; Geiser, L.; Svec, F.; Fréchet, J.; Rozing, G.; Shoenmakers, P.; Kok, W. Controlling the surface chemistry and chromatographic properties of methacrylate-ester based monolithic capillary columns via photografting. *J. Sep. Sci.* **2007**, *30*, 407–413.

68. Peterson, D.; Rohr, T.; Svec, F.; Fréchet, J. Dual-function microanalytical device by *in situ* photolithographic grafting of porous polymer monolith: Integrating solid-phase extraction and enzymatic digestion for peptide mass mapping. *Anal. Chem.* **2003**, *75*, 5328–5335.

69. Connolly, D.; Paull, B. High-performance separation of small inorganic anions on a methacrylate-based polymer monolith grafted with (2(methacryloyloxy)ethyl) trimethylammonium chloride. *J. Sep. Sci.* **2009**, *32*, 2653–2658.

70. Connolly, D.; O' Shea, V.; Clark, P.; O'Connor, B.; Paull, B. Evaluation of photografted charged sites within polymer monoliths in capillary columns using contactless conductivity detection. *J. Sep. Sci.* **2007**, *30*, 3060–3068.

71. Křenková, J.; Lacher, N.; Svec, F. Highly efficient enzyme reactors containing trypsin and endoproteinase lysc immobilized on porous polymer monolith coupled to MS suitable for analysis of antibodies. *Anal. Chem.* **2009**, *81*, 2004–2012.

72. Křenková, J.; Lacher, N.; Svec, F. Multidimensional system enabling deglycosylation of proteins using a capillary reactor with peptide-N-glycosidase F immobilized on a porous polymer monolith and hydrophilic interaction liquid chromatography–mass spectrometry of glycans. *J. Chromatogr. A* **2009**, *1216*, 3252–3259.

73. Potter, O.; Breadmore, M.; Hilder, E. Boronate functionalised polymer monoliths for microscale affinity chromatography. *Analyst* **2006**, *131*, 1094–1096.

74. Gillespie, E.; Connolly, D.; Nesterenko, P.; Paull, B. Accurate non-invasive determination of pK_a of surface functionalised ion exchange monoliths using capacitively coupled contactless conductivity detection. *Analyst* **2008**, *133*, 874–876.

75. Gillespie, E.; Connolly, D.; Nesterenko, P.; Paull, B. On-column titration and investigation of metal complex formation for aminopolycarboxylate functionalised monoliths using scanning contactless conductivity detection. *J. Sep. Sci.* **2009**, *32*, 2659–2667.

76. Walsh, Z.; Levkin, P.; Jain, V.; Paull, B.; Svec, F.; Macka, M. Visible light initiated polymerization of styrenic monolithic stationary phases using 470 nm light emitting diode arrays. *J. Sep. Sci.* **2010**, *33*, 61–66.

77. Walsh, Z.; Levkin, P.; Abele, S.; Scarmagnani, S.; Heger, D.; Klán, P.; Diamond, D.; Paull, B.; Svec, F.; Macka, M. Polymerisation and surface modification of methacrylate monoliths in polyimide channels and polyimide coated capillaries using 660 nm light emitting diodes. *J. Chromatogr. A* **2011**, *1218*, 2954–2962.

78. Moyna, A.; Connolly, D.; Nesterenko, E.; Nesterenko, P.; Paull, B. Separation of selected transition metals by capillary chelation ion chromatography using acetyl-iminodiacetic acid modified capillary polymer monoliths. *J. Chromatogr. A* **2012**, *1249*, 155–163.

79. Moyna, A.; Connolly, D.; Nesterenko, E.; Nesterenko, P.; Paull, B. Iminodiacetic acid functionalised organopolymer monoliths: Application to the separation of metal cations by capillary high-performance chelation ion chromatography. *Anal. Bioanal. Chem.* **2013**, *405*, 2207–2217.

80. Rohr, T.; Ogletree, D.; Svec, F.; Fréchet, J. Surface functionalization of thermoplastic polymers for the fabrication of microfluidic devices by photoinitiated grafting. *Adv. Funct. Mater.* **2003**, *13*, 264–270.

81. Keppler, M.; Hüsing, N. Space-confined click reactions in hierarchically organized silica monoliths. *New J. Chem.* **2011**, *35*, 681–690.

82. Slater, M.; Fréchet, J.; Svec, F. In-column preparation of a brush-type chiral stationary phase using click chemistry and a silica monolith. *J. Sep. Sci.* **2009**, *32*, 21–28.

83. Keppler, M.; Holzbock, J.; Akbarzadeh, J.; Peterlik, H.; Hüsing, N. Inorganic–organic hybrid materials through postsynthesis modification: Impact of the treatment with azides on the mesopore structure. *Beilstein J. Nanotechnol.* **2011**, *2*, 486–498.

84. Chen, Y.; Wu, M.; Wang, K.; Chen, B.; Yao, S.; Zou, H.; Nie, L. Vinyl functionalized silica hybrid monolith-based trypsin microreactor for on line digestion and separation via thiol-ene "click" strategy. *J. Chromatogr. A* **2011**, *1218*, 7982–7988.

85. Wang, K.; Chen, Y.; Yang, H.; Li, Y.; Nie, L.; Yao, S. Modification of VTMS hybrid monolith via thiol-ene click chemistry for capillary electrochromatography. *Talanta* **2012**, *91*, 52–59.

86. Yang, H.; Chen, Y.; Liu, Y.; Nie, L.; Yao, S. One-pot synthesis of (3-sulfopropyl methacrylate potassium)-silica hybrid monolith via thiol-ene click chemistry for CEC. *Electrophoresis* **2013**, *34*, 510–517.

87. Preinerstorfer, B.; Bicker, W.; Linder, W.; Lämmerhofer, M. Development of reactive thiol-modified monolithic capillaries and in-column surface functionalization by radical addition of a chromatographic ligand for capillary electrochromatography. *J. Chromatogr. A* **2004**, *1044*, 187–199.

88. Lv, Y.; Hughes, T.; Hao, X.; Hart, N.; Littler, S.; Zhang, X.; Tan, T. A novel route to prepare highly reactive and versatile chromatographic monoliths. *Macromol. Rapid Commun.* **2010**, *31*, 1785–1790.

89. Lv, Y.; Lin, Z.; Svec, F. ''Thiol–ene'' click chemistry: A facile and versatile route for the functionalization of porous polymer monoliths. *Analyst* **2012**, *137*, 4114–4118.

90. Tijunelyte, I.; Babinot, J.; Guerrouache, M.; Valincius, G.; Carbonnier, B. Hydrophilic monolith with ethylene glycol-based grafts prepared via surface confined thiol-ene click photoaddition. *Polymer* **2012**, *53*, 29–36.

91. Sun, X.; Lin, D.; He, X.; Chen, L.; Zhang, Y. A facile and efficient strategy for one-step *in situ* preparation of hydrophobic organic monolithic stationary phases by click chemistry and its application on protein separation. *Talanta* **2010**, *82*, 404–408.

92. Sun, X.; He, X.; Chen, L.; Zhang, Y. In-column "click" preparation of hydrophobic organic monolithic stationary phases for protein separation. *Anal. Bioanal. Chem.* **2011**, *399*, 3407–3413.

93. Salwinski, A.; Roy, V.; Agrofoglio, L.; Delépée, R. *In situ* one-step method for synthesis of "click"-functionalized monolithic stationary phase for capillary electrochromatography. *Macromol. Chem. Phys.* **2011**, *212*, 2700–2707.

94. Viklund, C.; Svec, F.; Fréchet, J.; Irgum, K. Fast ion-exchange HPLC of proteins using porous poly(glycidyl methacrylate-co-ethylene dimethacrylate) monoliths grafted with poly(2-acrylamido-2-methyl-1-propanesulfonic acid). *Biotechnol. Prog.* **1997**, *13*, 597–600.

95. Viklund, C.; Irgum, K. Synthesis of porous zwitterionic sulfobetaine monoliths and characterization of their interaction with proteins. *Macromolecules.* **2000**, *33*, 2539–2544.

96. Meyer, U.; Svec, F.; Fréchet, J.; Hawker, C.; Irgum, K. Use of stable free radicals for the sequential preparation and surface grafting of functionalized macroporous monoliths. *Macromolecules* **2000**, *33*, 7769–7775.

97. Georges, M.; Veregin, R.; Kazmaier, P.; Hamer, G. Narrow molecular weight resins by a free-radical polymerisation process. *Macromolecules* **1993**, *26*, 2987–2988.

98. Buchmeiser, M.; Sinner, F.; Mupa, M.; Wurst, K. Ring-opening metathesis polymerization for the preparation of surface-grafted polymer supports. *Macromolecules* **2000**, *33*, 32–39.

99. Sinner, F.; Buchmeiser, M. A new class of continuous polymer supports prepared by ring-opening metathesis polymerization: A straightforward route to functionalized monoliths. *Macromolecules* **2000**, *33*, 5777–5786.

100. Kanamori, K.; Hasegawa, J.; Nakanishi, K.; Hanada, T. Facile synthesis of macroporous cross-linked methacrylate gels by atom transfer radical polymerization. *Macromolecules* **2008**, *41*, 7186–7193.

101. Limé, F.; Irgum, K. Hydrobromination of residual vinyl groups on divinylbenzene polymer particles followed by atom transfer radical surface graft polymerization. *J. Polym. Sci.: Part A: Polym. Chem.* **2009**, *47*, 1259–1265.

102. Liu, H.; Zhuang, X.; Turson, M.; Zhang, M.; Dong, X. Enrofloxacin-imprinted monolithic columns synthesized using reversible addition-fragmentation chain transfer polymerization. *J. Sep. Sci.* **2008**, *31*, 1694–1701.

103. Barlow, K.; Hao, X.; Hughes, T.; Hutt, O.; Polyzos, A.; Turner, K.; Moad, G. Porous, functional poly(styrene-co-divinylbenzene) monoliths by RAFT polymerization. *Polym. Chem.* **2014**, *5*, 722–732.

104. Viklund, C.; Nordström, A.; Irgum, K.; Svec, F.; Fréchet, J. Preparation of porous poly (styrene-co-divinylbenzene) monoliths with controlled pore size distributions initiated by stable free radicals and their pore surface functionalization by grafting. *Macromolecules* **2001**, *34*, 4361–4369.

105. Peters, E.; Svec, F.; Fréchet, J.; Viklund, C.; Irgum, K. Control of porous properties and surface chemistry in "molded" porous polymer monoliths prepared by polymerization in the presence of TEMPO. *Macromolecules.* **1999**, *32*, 6377–6379.

106. Germain, J.; Fréchet, J.; Svec, F. Nanoporous, hypercrosslinked polypyrroles: Effect of crosslinking moiety on pore size and selective gas adsorption. *Chem. Commun.* **2009**, doi:10.1039/B821233C.

107. Davankov, V.; Rogozhin, S.; Tsyurupa, M. Macronet Polystyrene Structures for Ionites and Method of Producing Same. U.S. Patent 3,729,457, 24 April 1973.

108. Pastukhov, A.; Tsyurupa, M.; Davankov, V. Hypercrosslinked polystyrene: A polymer in a non-classical physical state. *J. Polym. Sci. Polym. Phys.* **1999**, *37*, 2324–2333.

109. Davankov, V.; Tsyurupa, M. Structure and properties of hypercrosslinked polystyrene—The first representative of a new class of polymer networks. *React. Polym.* **1990**, *13*, 27–42.

110. Davankov, V.; Tsyurupa, M.; Ilyin, M.; Pavlova, L. Hypercross-linked polystyrene and its potentials for liquid chromatography: A mini-review. *J. Chromatogr. A* **2002**, *965*, 65–73.

111. Tsyurupa, M.; Davankov, V. Porous structure of hypercrosslinked polystyrene: State-of-the-art mini-review. *React. Funct. Polym.* **2006**, *66*, 768–779.

112. Urban, J.; Svec, F.; Fréchet, J. Efficient separation of small molecules using a large surface area hypercrosslinked monolithic polymer capillary column. *Anal. Chem.* **2010**, *82*, 1621–1623.

113. Minakuchi, H.; Nakanishi, K.; Soga, N.; Ishizuka, N.; Tanaka, N. Octadecylsilylated porous silica rods as separation media for reversed-phase liquid chromatography. *Anal. Chem.* **1996**, *68*, 3498–3501.

114. Urban, J.; Svec, F.; Fréchet, J. Hypercrosslinking: New approach to porous polymer monolithic capillary columns with large surface area for the highly efficient separation of small molecules. *J. Chromatogr. A* **2010**, *1217*, 8212–8221.

115. Chen, X.; Dinh, N.; Zhao, J.; Wang, Y.; Li, S.; Svec, F. Effect of ion adsorption on CEC separation of small molecules using hypercrosslinked porous polymer monolithic capillary columns. *J. Sep. Sci.* **2012**, *35*, 1502–1505.

116. Teisseyre, T.; Urban, J.; Halpern-Manners, N.; Chambers, S.; Bajaj, V.; Svec, F.; Pines, A. Remotely detected NMR for the characterization of flow and fast chromatographic separations using organic polymer monoliths. *Anal. Chem.* **2011**, *83*, 6004–6010.

117. Škeříková, V.; Urban, J. Highly stable surface modification of hypercrosslinked monolithic capillary columns and their application in hydrophilic interaction chromatography. *J. Sep. Sci.* **2013**, *36*, 2806–2812.

118. Lv, Y.; Lin, Z.; Svec, F. Hypercrosslinked large surface area porous polymer monoliths for hydrophilic interaction liquid chromatography of small molecules featuring zwitterionic functionalities attached to gold nanoparticles held in layered structure. *Anal. Chem.* **2012**, *84*, 8457–8460.

119. Křenková, J.; Foret, F. Iron oxide nanoparticle coating of organic polymer-based monolithic columns for phosphopeptide enrichment. *J. Sep. Sci.* **2011**, *34*, 2106–2112.

120. Li, Y.; Chen, Y.; Xiang, R.; Ciuparu, D.; Pfefferle, L.; Horvath, C.; Wilkins, J. Incorporation of single-wall carbon nanotubes into an organic polymer monolithic stationary phase for μ-HPLC and capillary electrochromatography. *Anal. Chem.* **2005**, *77*, 1398–1406.

121. Křenková, J.; Lacher, N.; Svec, F. Control of selectivity via nanochemistry: Monolithic capillary column containing hydroxyapatite nanoparticles for separation of proteins and enrichment of phosphopeptides. *Anal. Chem.* **2010**, *82*, 8335–8341.

122. Chambers, S.; Holcombe, T.; Svec, F.; Fréchet, J. Porous polymer monoliths functionalized through copolymerization of a C60 fullerene-containing methacrylate monomer for highly efficient separations of small molecules. *Anal. Chem.* **2011**, *83*, 9478–9484.

123. Tong, S.; Liu, Q.; Li, Y.; Zhou, W.; Jia, Q.; Duan, T. Preparation of porous polymer monolithic column incorporated with graphene nanosheets for solid phase microextraction and enrichment of glucocorticoids. *J. Chromatogr. A* **2012**, *1253*, 22–31.

124. Tobal, K.; Guerre, O.; Rolando, C.; Le Gac, S. Metal nanoparticle-based polymer monolithic columns dedicated to the specific trapping of phosphopeptides. *Mol. Cell. Proteomics* **2006**, *5*, S278.

125. Hsieh, H.; Sheu, C.; Shi, F.; Li, D. Development of a titanium dioxide nanoparticle pipette-tip for the selective enrichment of phosphorylated peptides. *J. Chromatogr. A* **2007**, *1165*, 128–135.

126. Rainer, M.; Sonderegger, H.; Bakry, R.; Huck, C.; Morandell, S.; Huber, L.; Gjerde, D.; Bonn, G. Analysis of protein phosphorylation by monolithic extraction columns based on poly(divinylbenzene) containing embedded titanium dioxide and zirconium dioxide nano-powders. *Proteomics* **2008**, *8*, 4593–4602.

127. Liu, J.; White, I.; DeVoe, D. Nanoparticle-functionalized porous polymer monolith detection elements for surface-enhanced raman scattering. *Anal. Chem.* **2011**, *83*, 2119–2124.

128. Lei, W.; Zhang, L.; Wan, L.; Shi, B.; Wang, Y.; Zhang, W. Hybrid monolithic columns with nanoparticles incorporated for capillary electrochromatography. *J. Chromatogr. A* **2012**, *1239*, 64–71.

129. Alwael, H.; Connolly, D.; Clarke, P.; Thompson, R.; Twamley, B.; O'Connor, B.; Paull, B. Pipette-tip selective extraction of glycoproteins with lectin modified gold nano-particles on a polymer monolithic phase. *Analyst* **2011**, *136*, 2619–2628.

130. Zhang, A.; Ye, F.; Lu, J.; Zhao, S. Screening α-glucosidase inhibitor from natural products by capillary electrophoresis with immobilized enzyme onto polymer monolith modified by gold nanoparticles. *Food Chem.* **2013**, *141*, 1854–1859.

131. Cao, Q.; Xu, Y.; Liu, F.; Svec, F.; Fréchet, J. Polymer monoliths with exchangeable chemistries: Use of gold nanoparticles as intermediate ligands for capillary columns with varying surface functionalities. *Anal. Chem.* **2010**, *82*, 7416–7421.

132. Guerrouache, M.; Mahouche-Chergui, S.; Chehimi, M.; Carbonnier, B. Site-specific immobilisation of gold nanoparticles on a porous monolith surface by using a thiol–yne click photopatterning approach. *Chem. Commun.* **2012**, *48*, 7486–7488.

133. Xu, Y.; Cao, Q.; Svec, F.; Fréchet, J. Porous polymer monolithic column with surface-bound gold nanoparticles for the capture and separation of cysteine-containing peptides. *Anal. Chem.* **2010**, *82*, 3352–3358.

134. Connolly, D.; Twamley, B.; Paull, B. High-capacity gold nanoparticle functionalised polymer monoliths. *Chem. Commun.* **2010**, *46*, 2109–2111.

135. Křenková, J.; Foret, F. Nanoparticle-modified monolithic pipette tips for phosphopeptide enrichment. *Anal. Bioanal. Chem.* **2013**, *405*, 2175–2183.

136. Li, W.; Zhou, X.; Ye, J.; Jia, Q. Develompent of a γ-alumina-nanoparticle functionalized porous polymer monolith for the enrichment of sudan dyes in red wine samples. *J. Sep. Sci.* **2013**, *36*, 3330–3337.

137. Floris, P.; Twamley B.; Nesterenko, P.; Paull, B.; Connolly, D. Agglomerated polymer monoliths with bimetallic nano-particles as flow-through micro-reactors. *Microchim. Acta* **2012**, *179*, 149–156.

138. Tong, S.; Zhou, X.; Zhou, C.; Li, Y.; Li, W.; Zhou, W.; Jia, Q. A strategy to decorate porous polymer monoliths with graphene oxide and graphene nanosheets. *Analyst* **2013**, *138*, 1549–1557.

139. Chambers, S.; Svec, F.; Fréchet, J. Incorporation of carbon nanotubes in porous polymer monolithic capillary columns to enhance the chromatographic separation of small molecules. *J. Chromatogr. A* **2011**, *1218*, 2546–2552.

140. Křenková, J.; Foret, F.; Svec, F. Less common applications of monoliths: V. Monolithic scaffolds modified with nanostructures for chromatographic separations and tissue engineering. *J. Sep. Sci.* **2012**, *35*, 1266–1283.

141. Nesterenko, E.; Nesterenko, P.; Connolly, D.; He, X.; Floris, P.; Duffy, E.; Paull, B. Nano-particle modified stationary phases for high-performance liquid chromatography. *Analyst* **2013**, *138*, 4229–4254.

142. Frens, G. Controlled nucleation for regulation of particle-size in monodisperse gold suspensions. *Nat. Phys. Sci.* **1973**, *241*, 20–22.